

UNCLASSIFIED

Defense Technical Information Center
Compilation Part Notice

ADP012383

TITLE: Modeling of the Gain, Temperature, and Iodine Dissociation Fraction in a Supersonic Chemical Oxygen-Iodine Laser

DISTRIBUTION: Approved for public release, distribution unlimited

This paper is part of the following report:

TITLE: Gas and Chemical Lasers and Intense Beam Applications III Held in San Jose, CA, USA on 22-24 January 2002

To order the complete compilation report, use: ADA403173

The component part is provided here to allow users access to individually authored sections of proceedings, annals, symposia, etc. However, the component should be considered within the context of the overall compilation report and not as a stand-alone technical report.

The following component part numbers comprise the compilation report:

ADP012376 thru ADP012405

UNCLASSIFIED

Modeling of the gain, temperature, and iodine dissociation fraction in a supersonic chemical oxygen-iodine laser

B. D. Barmashenko, E. Bruins, D. Furman, V. Rybalkin and S. Rosenwaks
Department of Physics, Ben-Gurion University of the Negev, Beer-Sheva 84105, Israel

ABSTRACT

We report on a simple one-dimensional model developed for the fluid dynamics and chemical kinetics in the chemical oxygen iodine laser (COIL). Two different I_2 dissociation mechanisms are tested against the performance of a COIL device in our laboratory. The two dissociation mechanisms chosen are the celebrated mechanism of Heidner and the newly suggested mechanism of Heaven. The gain calculated using Heaven's dissociation mechanism is much lower than the measured one. Employing Heidner's mechanism, a surprisingly good agreement is obtained between the measured and calculated gain and temperature over a wide range of the flow parameters. Other predictions of the model (larger mixing efficiency and higher temperature with a leak opened downstream of the resonator and gain decrease along the flow) are also in agreement with the experimental observations.

Keywords: chemical lasers, oxygen, iodine, power lasers

1. INTRODUCTION

The chemically driven oxygen iodine laser (COIL) ¹ is the only known example of a high power chemically driven electronic transition laser. The laser transition, at 1.315 microns, takes place between the spin-orbit levels of the ground state configuration of the iodine atom, $I(5p^5\ ^2P_{1/2}) \rightarrow I(5p^5\ ^2P_{3/2})$. The iodine atoms are pumped by a near resonant energy transfer from oxygen molecules in the excited singlet-delta state, $O_2(a^1\Delta_g)$



$O_2(^1\Delta)$ is produced in a chemical generator by the reaction of gaseous chlorine with a basic hydrogen peroxide solution (BHP). Mixing of the $O_2(^1\Delta)$ with I_2 molecules results in their dissociation to iodine atoms which are subsequently excited via reaction (1).

To understand the kinetic and mixing processes in COILs and optimize the output power it is necessary to have reliable models describing the COIL operation and, in particular, the small signal gain, iodine dissociation fraction and gas temperature in the resonator. One and quasi-two-dimensional models of supersonic COILs accounting for both chemical reactions and mixing processes were developed in ²⁻⁶. The calculated values of the power and gain are in reasonable agreement with experimental measurements performed for a small scale supersonic COIL developed in our laboratory ^{3, 7} and for the RADICL device, a 5 kW class supersonic COIL, developed at the Air Force Research Laboratory in Albuquerque, NM ^{8, 9}. More sophisticated three-dimensional (3-D) computational fluid dynamics (CFD) models were developed in ¹⁰⁻¹³ to take into account non-uniform distribution of the gain and temperature across the flow and, in particular, the three-dimensional horseshoe structure of the jets injected into the cross flow, shocks and turbulence that can not be directly modeled using the one and quasi-two-dimensional approaches. These 3-D models, however, are complex, need very long computation time and to the best of our knowledge are often inapplicable to parametric studies of the COIL when input parameters are changed continuously over a wide range. At the same time it appears that one- and quasi-two-dimensional models are able to reproduce most of the essential features of the chemical kinetics, mixing and hydrodynamics in the active medium of the COIL ^{5, 6}. Although these models give distributions of the small signal gain, temperature and density of $O_2(^1\Delta)$ only in the flow direction, the computation time is very short and it is possible to quickly predict performance over a wide range of input parameters (chemical flow rates, position of the mixing point and stagnation temperature). Since the values of some of the input parameters (the $O_2(^1\Delta)$ yield, flow rates of the

chlorine and water, stagnation temperature in the subsonic section of the flow and mixing efficiency) were previously known with very low accuracy it was very difficult to compare the results predicted by the aforementioned one-dimensional models with experimental data.

Recently we reported on diagnostic measurements in a slit nozzle supersonic COIL with transonic mixing, operating without primary buffer gas and with secondary N_2 ¹⁴. Using diode laser based diagnostics we measured the gain and temperature in the resonator, the $O_2(^1\Delta)$ yield and water vapor fraction in the subsonic section of the flow. In addition, the chlorine utilization and gas temperature at the generator exit were measured. In the present paper a simple one-dimensional model of the supersonic COIL with transonic injection of iodine is developed and used to simulate the experimental results obtained in¹⁴. This model is similar to the leaky stream tube model developed in³. The input parameters of the model were taken from the aforementioned measurements¹⁴. The objective of the present modeling is to provide for accurate calculations of chemical kinetics processes, rather than gas dynamics in the COIL. That is why most of the gas dynamics properties of the flow such as spatial distributions of the static pressure, static temperatures in the "cold" runs without chemical reactions, mixing efficiencies and stagnation pressures and temperatures, were also taken from the experiment. Calculations of the gain, temperature and iodine dissociation fraction along the flow as a function of the iodine flow rate, the most important parameter affecting both the gain and dissociation fraction, were carried out. The changes in iodine flow mainly affect the rates of chemical reactions and gas temperature and have only weak, indirect (via temperature changes) effect on the flow hydrodynamics. In particular, the iodine jets penetration into the primary flow (proportional to the momentum of the jet at the sonic injection hole and hence to the stagnation pressure of the secondary flow) is changed by less than 10-15% (depending on the iodine injector geometry) over the characteristic range of the iodine flow (0 – 0.4 mmole/s), which means that the iodine flow has a weak influence on the penetration. Our recent measurements¹⁵ of the gain distribution across the flow also confirm that the penetration is almost unaffected by the iodine flow. Indeed, for small values of the penetration parameter the gain distribution has bimodal structure with two peaks located higher and lower than the flow centerline and corresponding to the centerlines of the iodine jets. We observed that the peak positions and hence the iodine penetration, are almost independent of the iodine flow rate.

Comparison between the calculated and experimental dependencies of the gain and temperature on the iodine flow rate permits to determine which of the proposed kinetic schemes and sets of rate constants for I_2 dissociation,¹⁶ or¹⁷, fits better to the experimental results. The model was run for different flow rates of chlorine and secondary nitrogen and different positions of the optical axis along the flow and compared with the experimental results¹⁴.

2. OUTLINE OF THE MODEL

2.1 General assumptions of the model

The model considers a typical configuration of a supersonic COIL¹⁴ in which I_2 premixed with nitrogen (secondary flow) is injected perpendicularly into the main flow (primary flow) composed of O_2 [partially excited to $O_2(^1\Delta)$], H_2O and Cl_2 (see Fig. 1). The injection occurs in the transonic part of the supersonic slit nozzle through injection holes in each side (top and bottom). After the injection the gas is brought to supersonic velocity via expansion in the nozzle and flows through the duct with the floor and the ceiling diverging at an angle of 8° towards the optical resonator. As shown in² the perpendicular injection of the jets into the primary flow results in jets bending, merging of each series of single jets (injected from the same wall) to form a thin plane jet and jet-induced entrainment of some fraction of the primary gas into the jets. However, unlike our previous models^{2,3} the present model does not deal with the form and trajectory of the I_2/N_2 jets. Instead, just as in⁴ and⁶, an approach based on description of the injection and penetration processes by parallel streams is used. It is assumed that after the jets' bending is completed the two parallel streams are formed in the critical cross section of the nozzle, the O_2 primary stream and the mixed stream containing the entire I_2/N_2 secondary flow and fraction α_p of the primary flow instantly mixed with the secondary flow (see Fig. 2). In what follows this initial stage of mixing will be referred to as "premixing". Then the streams undergo supersonic expansion accompanied by chemical reactions in the mixed stream and gradual entrainment of the primary flow into the mixed stream (due to diffusion process). This process continues towards the optical resonator where the fraction of the primary flow entrained into the secondary stream due to diffusion process is indicated as β_p . The total mixing at the optical

axis is defined as the sum of α_p and β_p , determined below using the experimentally measured gain spatial profile across the flow. The model is divided into two main parts:

1. The first part of the model calculates the initial conditions in the primary and mixed streams at the critical cross section of the flow. The primary stream parameters before mixing with the secondary stream are equal to the critical flow parameters for Mach number equal to unity, the critical pressure of the primary flow being calculated from the measured stagnation pressure in the subsonic part of the flow. The stagnation pressure of the secondary flow before injection holes is found from the given flow rates of the iodine, nI_2 , nitrogen, nN_2 , and the stagnation temperature T_{s0} of the secondary flow, taking into account the injection holes discharge coefficient, $C_N \sim 0.7 - 0.8$ ¹⁸. The expansion of the jets is assumed to be adiabatic, but non-isentropic due to shock waves and viscosity. Due to irreversible effects, the stagnation pressure drops whereas the stagnation temperature remains unchanged for an adiabatic flow, the stagnation pressure losses PO_{L1} being 0.75- 0.9¹⁸. The exact value of PO_{L1} in this range has a very small effect on the calculated values of the gain and temperature. Parameters of the secondary stream before the “premixing” (temperature, velocity and cross section) are found from the given secondary flow rates, nI_2 and nN_2 , and the stagnation pressure (corrected by the loss factor PO_{L1}) and temperature of the secondary flow assuming equal static pressures in the primary and secondary streams. The secondary stream before the “premixing” is, as mentioned above, assumed to be parallel to the primary stream.

Flow parameters of the primary and mixed streams just after the “premixing” (see Fig. 1) are found from mass, momentum and energy conservation conditions assuming that the static pressure after premixing is equal to that before the “premixing”. The constant static pressure approximation during “premixing” is inaccurate since the pressure in the supersonic expansion changes rapidly away from the sonic line at the nozzle throat. However, this approximation has a very small effect on the calculations of the gain and temperature in the supersonic section of the flow because most of the chemical reactions start downstream of the throat.

2. In the second part of the model the mass flow rates $\omega_{m(p)}(Z)$ of species Z , the temperature $T_{m(p)}$ and the velocity $U_{m(p)}$ (the sub indexes “m” and “p” indicate mixed and primary streams, respectively) are calculated by solving the conservation differential equations, considering the supersonic expansion of the primary and mixed streams, the entrainment of the primary gas into the mixed layer and the chemical reactions occurring in the mixed layer. The final conditions of the primary and mixed streams after the “premixing”, as calculated in the first part of the model, serve as the initial conditions for the differential equations. In order to calculate the dynamical and chemical conditions at every point until the optical resonator, we assume a spatial dependence of the pressure along the flow. This dependence is based on the pressures measured at three points in the supersonic section of the flow and the critical pressure, calculated by the first part of the model. We assume the pressure to change linearly between successive points. In order to take into account non isentropic effects during the expansion in the slit nozzle (shock waves and boundary layers) we assumed that, just as for the jet expansion described in the first part of the model, the stagnation pressure in both the primary and secondary streams drops in the diverging section of the nozzle (from our calculations an exact position of the pressure drop location has a negligibly small effect on the calculated parameters). Like the loss factor PO_{L1} , the stagnation pressure loss factor PO_{L2} is 0.75- 0.9. It should be noted that with $PO_{L1(2)}$ equal to unity the calculated values of T_{mc} are smaller than the measured temperatures.

The above-mentioned first-order differential equations are solved numerically using “ode15s” Matlab computer program for stiff differential equations with relative error tolerance of 10^{-3} . The output of the program contains the values of the specific densities, temperature (T_m) and the flow parameters along the flow. The gain g and iodine dissociation fraction F are given by¹⁹

$$g = \frac{7}{12} \sigma ([I(^2P_{1/2})]_m - 0.5[I(^2P_{3/2})]_m), \quad (2)$$

and

$$F = 1 - \omega_m(I_2) / \omega_{m0}(I_2), \quad (3)$$

respectively, where $\sigma = 1.29 \times 10^{-17} (300/T_m)^{1/2} \text{ cm}^2$ is the stimulated emission cross section for the strongest transition $F = 3 \rightarrow F = 4$ between the hyperfine sublevels of the iodine atom and $\omega_{m0}(I_2)$ is the initial mass flow rate of I_2 before injection. Since the pressures at the optical axis are smaller than 2 Torr, Doppler approximation for the gain profile is used in Eq. (2). Running the program with different values of the input parameters gives the dependence of the gain, temperature and iodine dissociation fraction on these parameters.

2.2 Chemical reaction schemes

The model uses two different sets of chemical reactions suggested in ^{16, 17}. The first set of reactions is based on the mechanism of iodine dissociation suggested by Heidner et al. ¹⁶. This set of reactions was adopted in the standard kinetics package ^{20, 21} which is used for most computational simulations of COIL devices. Heidner's mechanism assumes that vibrationally excited $I_2(X)$ is the immediate precursor to atomic iodine in COIL systems and hence that the dissociation is a two step process requiring at least two $O_2(^1\Delta)$ molecules to dissociate one I_2 .

Recent kinetic measurements and modeling studies carried out by Heaven et al. ¹⁷ indicate that these assumptions are invalid, and that electronically excited $I_2(A')$ is the I atom precursor. Heaven et al. ¹⁷ suggested a new model of iodine dissociation where both $I_2(A')$ and vibrationally excited $I_2(X)$ are significant dissociation intermediates. This model requires at least three $O_2(^1\Delta)$ molecules to dissociate one I_2 . The second set of reactions used in our calculations is based on Heaven's mechanism of iodine dissociation.

3. CALCULATED RESULTS AND COMPARISON WITH EXPERIMENTAL MEASUREMENTS

3.1 Input parameters of the model

The input parameters of the model were measured in the experiment described in ¹⁴. Those parameters are the flow rates of the different species of primary and secondary flows, the temperature and pressure of both flows in the subsonic part and the pressure at three different points downstream of the supersonic nozzle exit plane. The cross-sections of the primary flow in the subsonic part (5 cm^2) and of the secondary flow in the sonic part (0.2 cm^2 and 0.34 cm^2 for transonic injectors No. 1 and 2, respectively, described in detail in ¹⁴), are fixed parameters.

There are three unknown parameters (explained in section 2.1) of the model: (1) the mixing parameter, α_p , or the total mixing efficiency $\eta_{mix} = \alpha_p + \beta_p$, (2) the losses in stagnation pressure of the secondary flow when injected into the primary flow, PO_{L1} , and (3) the losses in stagnation pressure of the flows during the supersonic expansion, PO_{L2} . The values of PO_{L1} and PO_{L2} are established in the following way: (a) the temperature of the gas mixture at the optical axis in the "cold runs", i. e., in the absence of iodine flow, is found by extrapolating the measured temperatures to nI_2 corresponding to zero gain as described in ¹⁴; (b) then, values for PO_{L1} and PO_{L2} are selected by which the calculated temperature of the mixed flow at the optical axis, for zero nI_2 , is equal to the extrapolated temperature. The previous procedure is based on the assumption that the iodine flow rate, which is very small compared to the total flow rate, does not affect the flow dynamics but has a strong effect on the chemical kinetics and hence the pressure losses for any nI_2 are the same as in the "cold runs". The parameter α_p is chosen to give the best fit to the experimental results. In section 3.3 we estimate the parameter α_p from experimental measurements of the gain spatial profile across the flow and compare it to the result obtained for α_p from the model. The input parameters of the model are shown in Table 1.

3.2 Comparison of calculated and experimental results

Figs. 3 and 4 show calculated dependencies of g , T_m and F on nI_2 for Heidner's and Heaven's mechanisms of iodine dissociation, respectively, for run 1 (Table 1) with $nCl_2 = 20$ mmole/s and the first position of the optical axis located 5 cm downstream of the injection point. The same figures show experimental dependencies of g and T_m on nI_2 obtained in ¹⁴. It should be mentioned that F is not measured during the experiment and therefore only the calculated results for F are presented. It is seen (Fig. 3) that a good agreement is obtained between the calculated and experimental results for the dissociation mechanism of Heidner. For the model including the dissociation mechanism of Heaven (Fig. 4) the gain obtained is much smaller than that measured in the same run. The reason for that is that the calculated values of F for Heaven's model are much smaller than for Heidner's model, e. g., for $nI_2 = 0.33$ mmole/s, corresponding to the maximum measured gain, the values of F are 0.4 and 0.76, for these models, respectively. Calculations show that good fit between the experimental and calculated results for Heaven's dissociation mechanism could not be obtained for other values (between 0 and 1) of the unknown input parameters of the model. In the remainder of this section we will use only the model which includes Heidner's mechanism.

In Fig. 3 the dashed lines are the gain and temperature calculated for large diffusion and as can be seen there is only a slight difference from the results calculated for small diffusion, the total mixing efficiency η_{mix} being the same for both cases. Therefore, from now on we will restrict ourselves to the case of small diffusion, which gives a slightly better fit.

Fig. 5 shows the gain and temperature as calculated for the second position of the optical axis, 9 cm downstream of the injection point, for the same conditions as in Figs. 3 and 4. As there are no sufficient experimental results for these conditions, only the calculated results are shown. Comparison between Fig. 5 and 3 shows that the gain decreases as the optical axis is moved downstream from the first position and the temperatures increase due to higher losses. This trend is also observed experimentally in ¹⁴.

Figs. 6 and 7 show that there is a good agreement between the calculated and experimental results for smaller values of nCl_2 (runs 2 and 3, Table 1). Fig. 8 shows the calculated and experimental results for an opened leak downstream of the cavity. As explained in ¹⁵, opening of the leak results in smaller pumping rate and Mach number in the cavity. It should be noted that to reach an agreement between the calculated and measured values of the gain we assumed (see Table 1) that the mixing efficiency η_{mix} for opened leak (~ 0.8) is larger than for closed leak (~ 0.5). This assumption is in good agreement with both estimates of η_{mix} using experimental measurements of the gain spatial profile across the flow presented below in section 3.3 and the conclusions of Ref. 14. The reason for larger mixing for opened leak is that the Mach number is smaller in this case, resulting in a larger time for mixing. It is worth noting that the values of the static pressure for opened leak are about 1.5 times larger than for closed leak due to higher back pressure introduced by the leak. Measurements of the pressure in the supersonic section of the flow show that the pressure decreases monotonically along the flow which means that there are no jumps in pressure caused by strong shock waves and only weak oblique shock waves may be present in the flow. These shock waves are therefore not taken into account in our one-dimensional model. Comparison between Fig. 8 and 3, 6 and 7 shows that the values of T_m and F for opened leak are higher than for closed leak, which is due to longer residence time of the flow between the injection point and the optical axis.

3.3 Estimate of the mixing parameter

To estimate the value of η_{mix} , experiments were carried out where the gain was measured as a function of the height y perpendicular to the direction of flow ¹⁵. Fig. 9 shows the dependencies $g(y)$ for the cases of closed and opened leak and the same flow conditions as in runs 1 and 4 (Table 1), respectively. It is seen that for the opened leak the gain is distributed more homogeneously along y than for closed leak.

η_{mix} can be defined as

$$\eta_{mix} \equiv \frac{\int_0^H g \cdot dy}{g_{max} H}, \quad (4)$$

where H is the height of the flow duct and g_{max} is the maximum value of the gain. Expression (4) does not take into account that the gain decreases near the walls not only because of the incomplete mixing but also due to increase in the gas temperature as a result of the heat transfer from the walls and wall deactivation of I^* . The later two processes occur in the thin boundary layers near the walls, hence Eq. (4) is a good approximation for η_{mix} ¹⁵. The values of η_{mix} estimated using Eq. (4) are 0.46 and 0.73 for closed and opened leak, respectively. These values are in excellent agreement with the values of η_{mix} used in the model, 0.48 (run 1) and 0.76 (run 4) for closed and opened leak, respectively.

4. SUMMARY

We tested the one-dimensional model presented in this paper against the performance of the COIL device in our laboratory. The celebrated Heidner's mechanism of iodine dissociation gives good agreement between the experimental and calculated results. The gain calculated using the newly suggested Heaven's dissociation mechanism is much lower than measured experimentally. It is shown that the rate of I_2 dissociation for Heaven's mechanism is smaller than that calculated using Heidner's mechanism. A possible reason is that the rate constants for Heaven's mechanism, obtained in¹⁷ by fitting the calculated to the experimentally measured times of iodine dissociation, are not accurate enough. It is worth noting that the set of rate constants given in¹⁷ are suggested to model the flow tube results of Heidner et al.¹⁶. This set, as noted in¹⁷, is not unique and may not model conditions of experiments with the supersonic COIL, lying outside the range of the data for which it was derived. Although good results are obtained for Heidner's mechanism, it suffers from inconsistencies, as discussed in¹⁷. It is very important therefore to measure experimentally the iodine dissociation fraction in order to decide which dissociation mechanism is closer to reality. But this is not an easy task as the absorption of I_2 molecules in the supersonic portion of the flow is very small, in particular when the gain length is short, as in our laser (5 cm).

The agreement obtained between the measured and calculated results over a wide range of the flow parameters is surprisingly good. Other predictions of the model (larger mixing efficiency and higher temperature with a leak opened downstream of the resonator and gain decrease along the flow) are also in agreement with the experimental observations.

REFERENCES

1. W. E. McDermott, N. R. Pchelkin, D. J. Benard and R. R. Bousek, "An electronic transition chemical laser," *Appl. Phys. Lett.*, vol. 32, pp. 469-470, 1978.
2. B. D. Barmashenko, A. Elijor, E. Lebiush and S. Rosenwaks, "Modeling of mixing in chemical oxygen-iodine lasers: Analytic and numerical solutions and comparison with experiments," *J. Appl. Phys.*, vol. 75, pp. 7653-7655, 1994.
3. A. Elijor, B. D. Barmashenko, E. Lebiush, and S. Rosenwaks, "Experiment and modeling of a small-scale, supersonic chemical oxygen-iodine laser," *Appl. Phys. B*, vol 61, pp. 37 - 47, 1995.
4. D. L. Carroll, "Modeling high-pressure chemical oxygen-iodine lasers," *AIAA Journal*, vol. 33, pp. 1454-1462, 1995.
5. B. D. Barmashenko and S. Rosenwaks, "Power dependence of chemical oxygen-iodine lasers on iodine dissociation," *AIAA J.*, vol. 34, pp. 2569-2574, 1996.
6. T. T. Yang, D. A. Copeland, A. H. Bauer, V. Quan, W. E. McDermott, R. A. Cover, D. M. Smith, "Chemical Oxygen-Iodine Laser Performance Modeling," in *AIAA 28th Plasmadynamics and Lasers Conf.*, Atlanta, GA, June 23-25, 1997, paper 97-2384.

7. E. Lebiush, B. D. Barmashenko, A. Elior and S. Rosenwaks, "Parametric study of the gain in a small scale, grid nozzle supersonic chemical oxygen-iodine laser," *IEEE J. Quantum Electronics*, vol.31, pp. 903-909, 1995.
8. C. A. Helms, J. Shaw, G. D. Hager and K. A. Truesdell, "Iodine dissociation in COILs," *SPIE*, vol. 2502, pp. 250 – 257, 1996.
9. R. F. Tate, B. S. Hunt, C. A. Helms, K. A. Truesdell and G. D. Hager, "Spatial gain measurements in a chemical oxygen iodine laser (COIL)," *IEEE J. Quantum Electronics*, vol.31, pp. 1632 - 1636, 1995.
10. T. G. Madden, W. C. Solomon, "A detailed comparison of a computational fluid dynamic simulation and a laboratory experiment for a COIL laser" in *AIAA 28th Plasmadynamics and Lasers Conf.*, Atlanta, GA, June 23-25, 1997, paper 97-2387.
11. T. G. Madden, G. D. Hager, A. I. Lampson and P. G. Crowell, "An investigation of supersonic mixing mechanism for the chemical oxygen-iodine laser (COIL)," in *AIAA 30th Plasmadynamics and Lasers Conf.*, Norfolk, VA, June 28- July 1, 1999, paper 99-3429.
12. W. Masuda, M. Hishida and N. Azami, "Mixing/reacting zone structure and small signal gain coefficient of a supersonic flow chemical oxygen-iodine laser," *SPIE*, vol. 3092, pp. 573 – 576, 1997.
13. M. Suzuki, T. Suzuki and W. Masuda, "Numerical simulation of throat-mixing system for supersonic flow chemical oxygen-iodine laser," *SPIE*, vol. 4184, pp. 99 – 102, 2001.
14. D. Furman, E. Bruins, V. Rybalkin, B. D. Barmashenko and S. Rosenwaks, "Parametric study of small signal gain in a slit nozzle, supersonic chemical oxygen - iodine laser operating without primary buffer gas," *IEEE J. Quantum Electronics*, vol. 37, pp. 174-182, 2001.
15. S. Rosenwaks, V. Rybalkin, E. Bruins, D. Furman, B. D. Barmashenko and A. Katz, "Spatial Distribution of the Gain and Temperature across the Flow in a Slit Nozzle Supersonic COIL with Different Schemes of Iodine Injection," presented at the COIL R&D Workshop Prague 2001, Prague, Czech Republic, 2001.
16. R. F. Heidner III, C. E. Gardner, G. I. Segal, , T. M. El-Sayed, "Chain reaction mechanism for I₂ dissociation in the O₂(¹Δ)-I atom laser," *Journal of Physical Chemistry*, vol. 87, pp. 2348-2360, 1983.
17. A. V. Kommisarov, V. Goncharov and M. C. Heaven, "Chemical oxygen iodine laser (COIL) kinetics and mechanisms," *SPIE*, vol. 4184, pp. 7 – 12, 2001.
18. A. H. Shapiro, *The Dynamics and Thermodynamics of Compressible Fluid Flow*. New York: Ronald, 1953, vol. 1, pp. 73-110.
19. N. N. Yuryshev, "Chemically pumped oxygen-iodine laser," *Quantum Electronics*, vol. 23, pp. 583 - 600, 1996.
20. G. P. Perram, "Approximate analytic solution for the dissociation of molecular iodine in the presence of singlet oxygen," *Int. J. Chem. Kinet.*, vol. 27, pp. 817-828, 1995.
21. G. P. Perram and G. D. Hager, "The standard chemical oxygen-iodine laser kinetics package," U. S. Air Force Weapons Lab., AFWL-TR-88-50, Kirtland AFB, NM, Oct. 1988.

Table 1. Input parameters of the model for different runs. The values are taken from the measurements of Ref. 14, except $P_{O_{L1}}$, $P_{O_{L2}}$ and η_{mix} which are fitting parameters

Run No. (Fig. No)	Nozzle type	nCl_2 [mmole/s]	nN_2 [mmole/s]	Leak	p_{sub}^* , [Torr]	p_{res}^* , [Torr]	Y	$P_{O_{L1}}$	$P_{O_{L2}}$	η_{mix}
1(3)	No. 2	20.1	8.7	closed	16.9	1.4	0.52	0.75	0.75	0.48
2(6)	No. 2	15.1	7.1	closed	12.7	1.1	0.56	0.75	0.85	0.51
3(7)	No. 2	11.8	5.1	closed	8.5	1	0.6	0.9	0.9	0.6
4(8)	No.1	11.7	3	opened	8.7	1.4	0.5	0.75	0.75	0.76

*Pressure measured in the subsonic section of the flow.

** Pressure measured at the optical axis of the resonator.

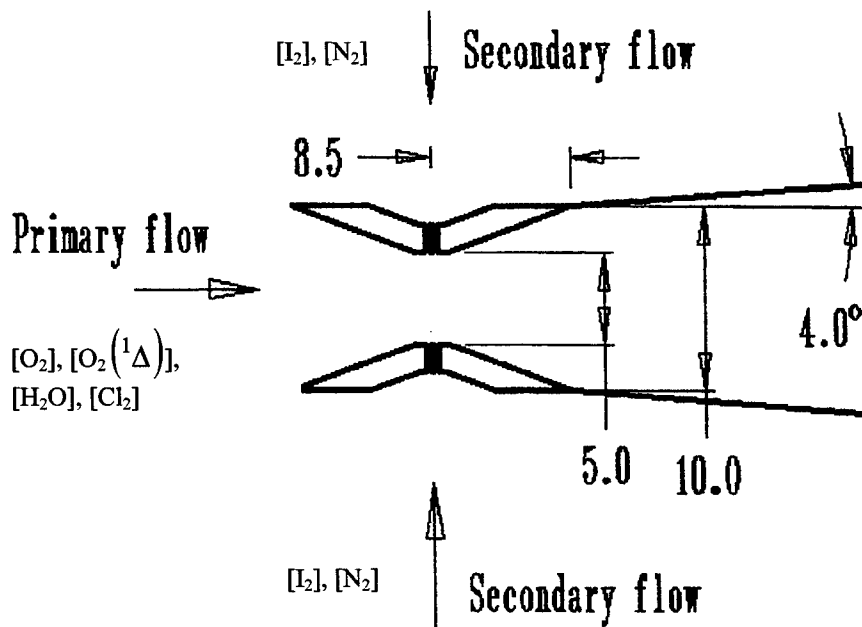


Fig. 1 Schematic of the supersonic nozzle with transonic injection of I_2 (measures are in millimeters).

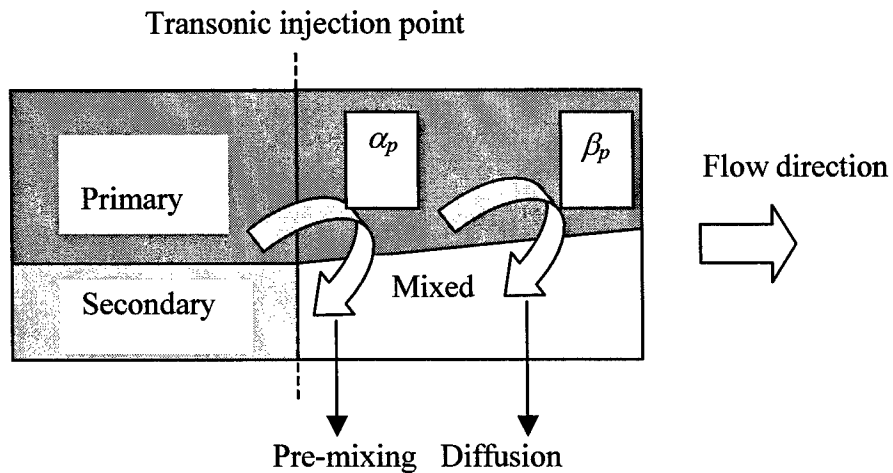


Fig. 2 Schematic of the mixing concept in the model. α_p is the fraction of the primary flow "premixed" with the secondary flow; β_p is the fraction of the primary flow at the optical axis obtained due to gradual mixing with the secondary flow during the supersonic expansion.

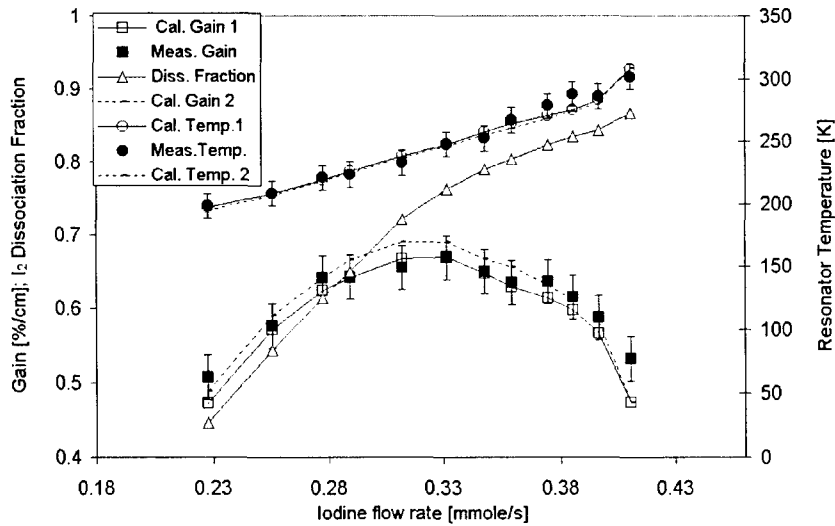


Fig. 3 Calculated (using Heidner's model) and measured gain g , temperature T_m and iodine dissociation fraction F at the first position of the cavity optical axis (5 cm downstream of the injection point) as a function of the iodine flow rate. The chlorine and secondary nitrogen flow rates are 11.7 and 8.7 mmole/s, respectively, the leak downstream of the cavity is closed (run No. 1, Table 1). Calculated gains and temperatures indicated by 1 (solid line) and 2 (dashed line) correspond to the slow and fast diffusion, respectively, the total mixing efficiency η_{mix} being the same for both cases.

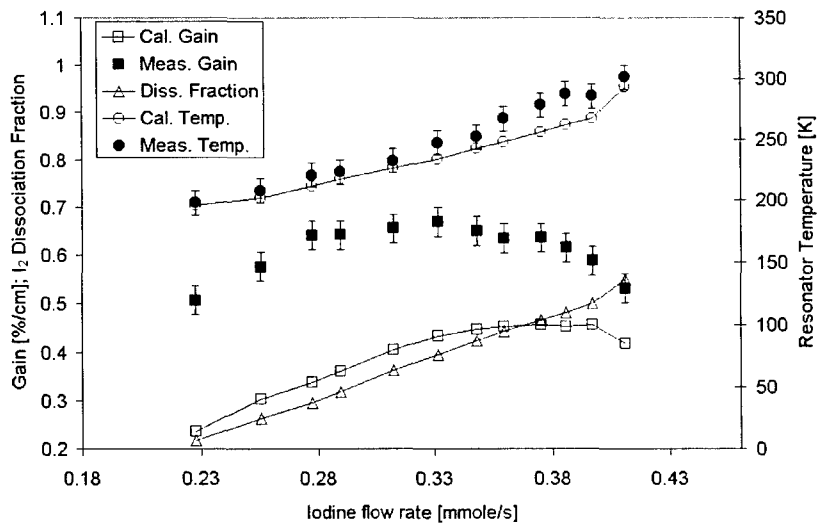


Fig. 4 Calculated (using Heaven's model) and measured gain g , temperature T_m and iodine dissociation fraction F for the same conditions as in Fig. 3 (run No. 1, Table 1)

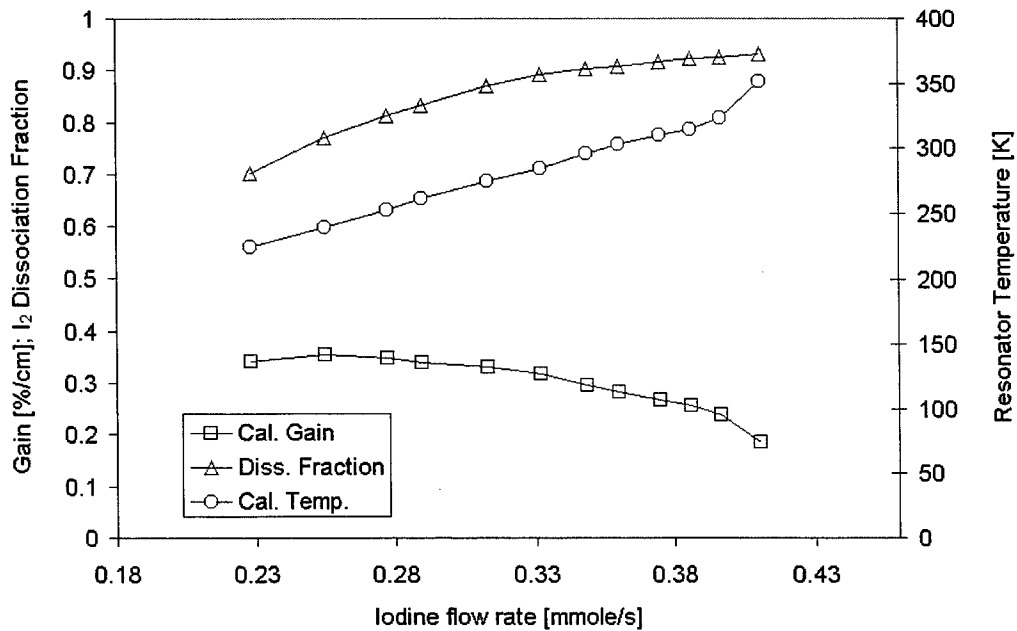


Fig. 5 Calculated (using Heidner's model) gain g , temperature T_m and iodine dissociation fraction F at the second position of the cavity optical axis (9 cm downstream of the injection point) for the same conditions as in Fig. 3 (run No. 1, Table 1)

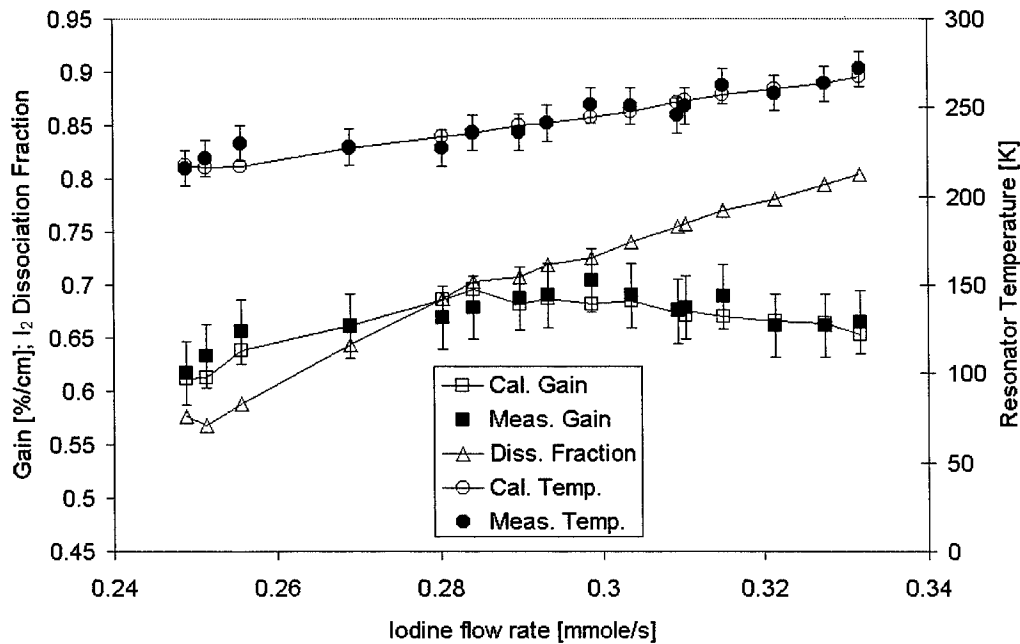


Fig. 6 Calculated (using Heidner's model) and measured gain g , temperature T_m and iodine dissociation fraction F at the first position of the cavity optical axis (5 cm downstream of the injection point) as a function of the iodine flow rate. The chlorine and secondary nitrogen flow rates are 15.1 and 7.1 mmole/s, respectively, the leak downstream of the cavity is closed (run No. 2, Table 1)

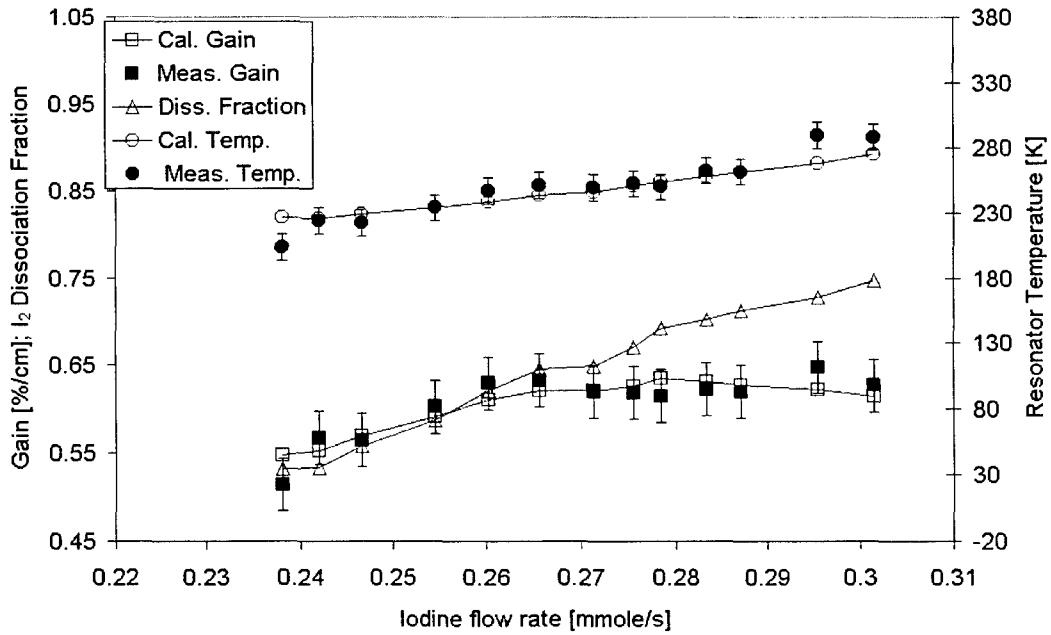


Fig. 7 Calculated (using Heidner's model) and measured gain g , temperature T_m and iodine dissociation fraction F at the first position of the cavity optical axis (5 cm downstream of the injection point) as a function of the iodine flow rate. The chlorine and secondary nitrogen flow rates are 11.8 and 5.1 mmole/s, respectively, the leak downstream of the cavity is closed (run No. 3, Table 1)

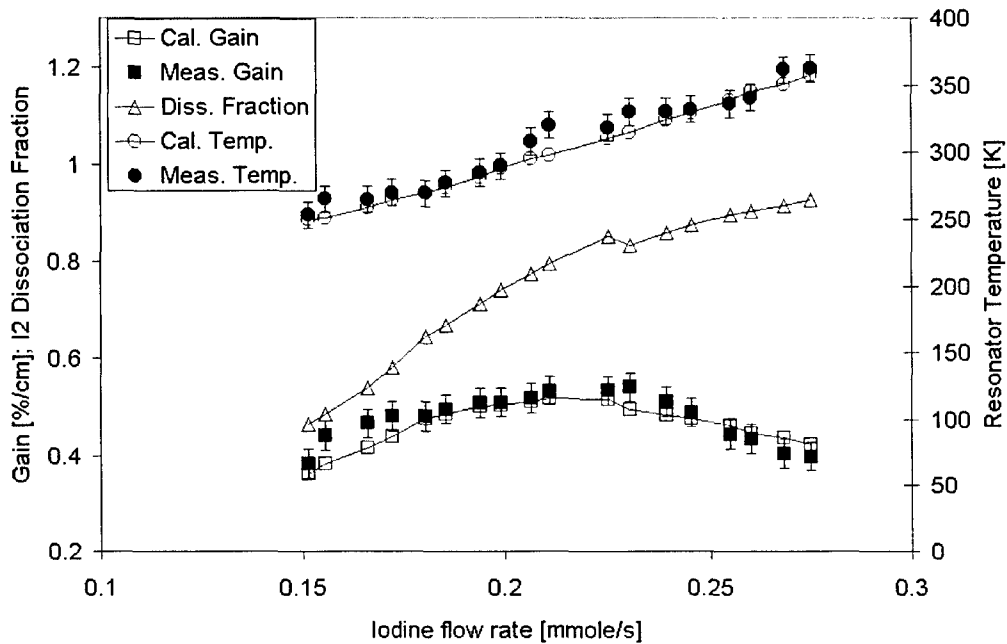


Fig. 8 Calculated (using Heidner's model) and measured gain g , temperature T_m and iodine dissociation fraction F at the first position of the cavity optical axis (5 cm downstream of the injection point) as a function of the iodine flow rate. The chlorine and secondary nitrogen flow rates are 11.7 and 3 mmole/s, respectively, the leak downstream of the cavity is opened (run No. 4, Table 1).

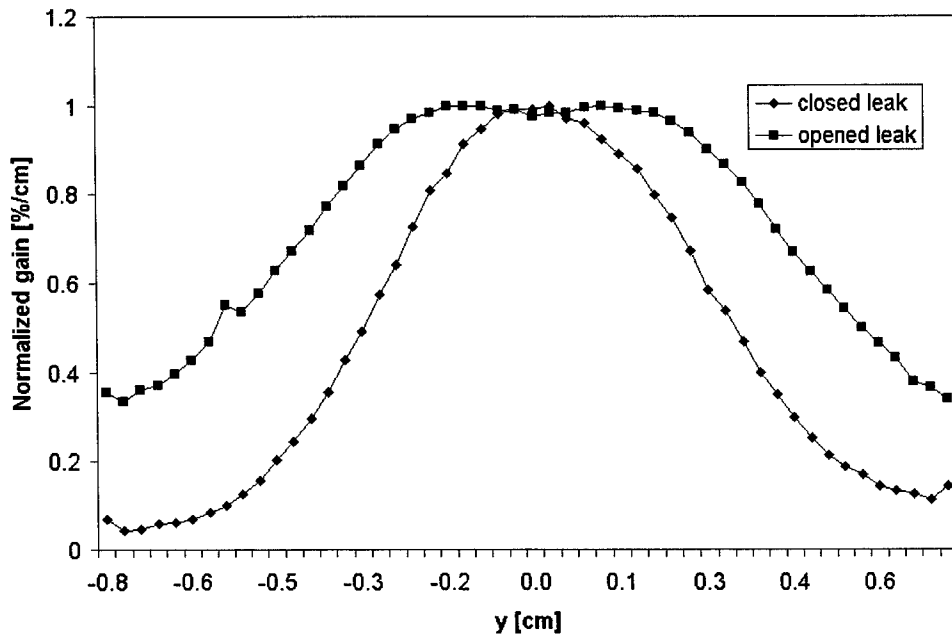


Fig. 9 Measured gain distribution in the y direction across the flow for closed and opened leak.